Separation Science and Technology
Publication details, including instructions for authors and subscription information:
http://www.informaworld.com/smpp/title~content=t713708471

Experimental and Numerical Investigation of Adsorption/Desorption in Packed Sorption Beds under Ideal and Nonideal Flows

H. Mohamadinejad[a]; J. C. Knox[b]; James E. Smith[c]
[a] BOEING AEROSPACE COMPANY, HUNTSVILLE, ALABAMA, USA [b] MARSHALL SPACE FLIGHT CENTER, NATIONAL AERONAUTICS AND SPACE ADMINISTRATION, HUNTSVILLE, ALABAMA, USA [c] DEPARTMENT OF CHEMICAL ENGINEERING, UNIVERSITY OF ALABAMA IN HUNTSVILLE, HUNTSVILLE, ALABAMA, USA

Online publication date: 01 April 2000

To cite this Article Mohamadinejad, H. , Knox, J. C. and Smith, James E.(2000) 'Experimental and Numerical Investigation of Adsorption/Desorption in Packed Sorption Beds under Ideal and Nonideal Flows', Separation Science and Technology, 35: 1, 1 — 22
To link to this Article: DOI: 10.1081/SS-100100140
URL: http://dx.doi.org/10.1081/SS-100100140

SEPARATION SCIENCE AND TECHNOLOGY, **35**(1), pp. 1–22, 2000

Experimental and Numerical Investigation of Adsorption/Desorption in Packed Sorption Beds under Ideal and Nonideal Flows

H. MOHAMADINEJAD
BOEING AEROSPACE COMPANY
HUNTSVILLE, ALABAMA, USA

J. C. KNOX
MARSHALL SPACE FLIGHT CENTER
NATIONAL AERONAUTICS AND SPACE ADMINISTRATION
HUNTSVILLE, ALABAMA, USA

JAMES E. SMITH, Ph.D.*
DEPARTMENT OF CHEMICAL ENGINEERING
UNIVERSITY OF ALABAMA IN HUNTSVILLE
HUNTSVILLE, ALABAMA, USA

ABSTRACT

The importance of the wall effect on packed beds in the adsorption and desorption of carbon dioxide, nitrogen, and water on molecular sieve 5A of 0.127 cm radius is examined experimentally and with one-dimensional computer simulations. Experimental results are presented for a 22.5-cm long by 4.5-cm diameter cylindrical column with concentration measurements taken at various radial locations. The set of partial differential equations is solved using finite differences and Newmans's method. Comparison of test data with the axial-dispersed, nonisothermal, linear driving force model suggests that a two-dimensional model (submitted to *Separation Science and Technology*) is required for accurate simulation of the average column breakthrough concentration. Additional comparisons of test data with the model provided information on the interactive effects of carrier gas coadsorption with CO_2 as well as CO_2–H_2O interactions.

* To whom correspondence should be addressed.

INTRODUCTION

The presence of the confining walls in a packed bed can have a significant influence on the axial flow and therefore heat and mass transfer in the packed bed. The viscous shear force along the wall and the increase in porosity near the wall can have opposing effects on overall permeability. For values of tube-to-particle diameter ratio, *R*, less than about 7, the permeability has been shown to increase above that of an infinite porous medium (1–3). Between *R* values of 7 and 30, variations in bed packing may determine the governing influence. For *R* values above 30, the influence is generally considered insignificant (3), although it was found to be important for an *R* value greater than 100 in an adsorption study by Tobis and Vortmeyer (4).

Wall effects on packed-bed processes can be significant in heat and mass transfer driven processes, since the value of *R* is frequently within this sensitivity range. Examples are thermal swing adsorption beds where a heater matrix results in small rectangular columns, wall-cooled catalytic reactors (5), and packed-bed energy storage units (6).

In this work we examine the influence of wall effects on mass and heat transfer during adsorption and desorption in a packed column. The experimental results for carbon dioxide and water adsorption in a nitrogen carrier gas provide information on the sensitivity of the adsorption to wall effects in a column with an intermediate tube-to-particle diameter ratio, *R*, of 15. Adsorption breakthrough data are presented for various radial locations at the bed exit, which can be used as a measure of permeability or channeling along the column wall.

A computer model was developed based on the finite-differencing numerical technique. The model simulates gas adsorption and desorption in a flow-through bed. Single and multicomponent adsorption; thermal balances for the pellet, gas, and canister; and the momentum equation are included. A two-dimensional (radial and axial) model was also developed to predict the effect of flow channeling on adsorption and desorption. It is described in a later paper (7).

EXPERIMENTAL APPARATUS AND RESULTS

Adsorption Test System

The test flow rate was scaled to give gas velocities similar to that in the proposed flight beds for the International Space Station Carbon Dioxide Removal Assembly. Instrumentation of the packed column includes temperature probes and sampling tubes for measurements at sorbent material endpoints and one intermediate point. To attain approximately adiabatic bed conditions, the col-

umn was first covered with Mansfield Q-fiber felt insulation, then wrapped with a thermal blanket of Mansfield Min-K material. For adsorption runs, an additional jacket fabricated of STS External Tank insulating foam was attached. The insulation, approximately 3 inches thick in all, was used with satisfactory results.

Instrumentation was provided for continuous measurement of packed column outlet CO_2 and H_2O concentration. The locations of sensors and other equipment comprising the adsorbing apparatus are shown in Fig. 1. The column bypass is used prior to the test start to ensure stable column inlet conditions.

The gas chromatograph, a Shimadzu GC-14A with CR601 integrator, was used at three sample port locations to determine gas constituent volumetric fractions during the adsorption runs. The probe depth of the sampling tube at the column exit was adjusted to obtain a radial profile of the exit concentration during a series of identical CO_2 adsorption tests.

Column Dynamics Test Bed

A small packed column with approximate dimensions of 2 inches in diameter and 20 inches long (Fig. 2) located at Marshall Space Flight Center was used. The column may be packed with up to 20 inches of sorbent. A 10-inch packing was used in this study for quicker results and reduced thermal end effects. Placing 4.75 inches of glass beads at the two ends of the column eliminated the end effects.

Procedure

Experiments were performed on the insulated fixed-bed rig at MSFC. The sorbent was a 5A zeolite. Nitrogen was the carrier gas. Experiments begin with the column at ambient room temperature. The column bypass shown in Fig. 1 was used to obtain intended inlet conditions before exposure of the column to the inlet gas. The GC sampling location was switched during the test to follow the sorbate mass transfer wave as it proceeded down the bed.

Results and Discussion

Figure 3 shows the water breakthrough at the column midpoint and outlet. Also shown is the H_2O partial pressure of gas mixed by passing through glass beads downstream of the sorbent material. Note the mixed gas breaks through before the gas at the centerline, indicating that channeling has a significant effect on the process efficiency for the 2-inch diameter column.

To provide a measure of the radial variation in axial flow, adsorption tests of CO_2 and N_2 were conducted repeatedly with the exit sampling tube in dif-

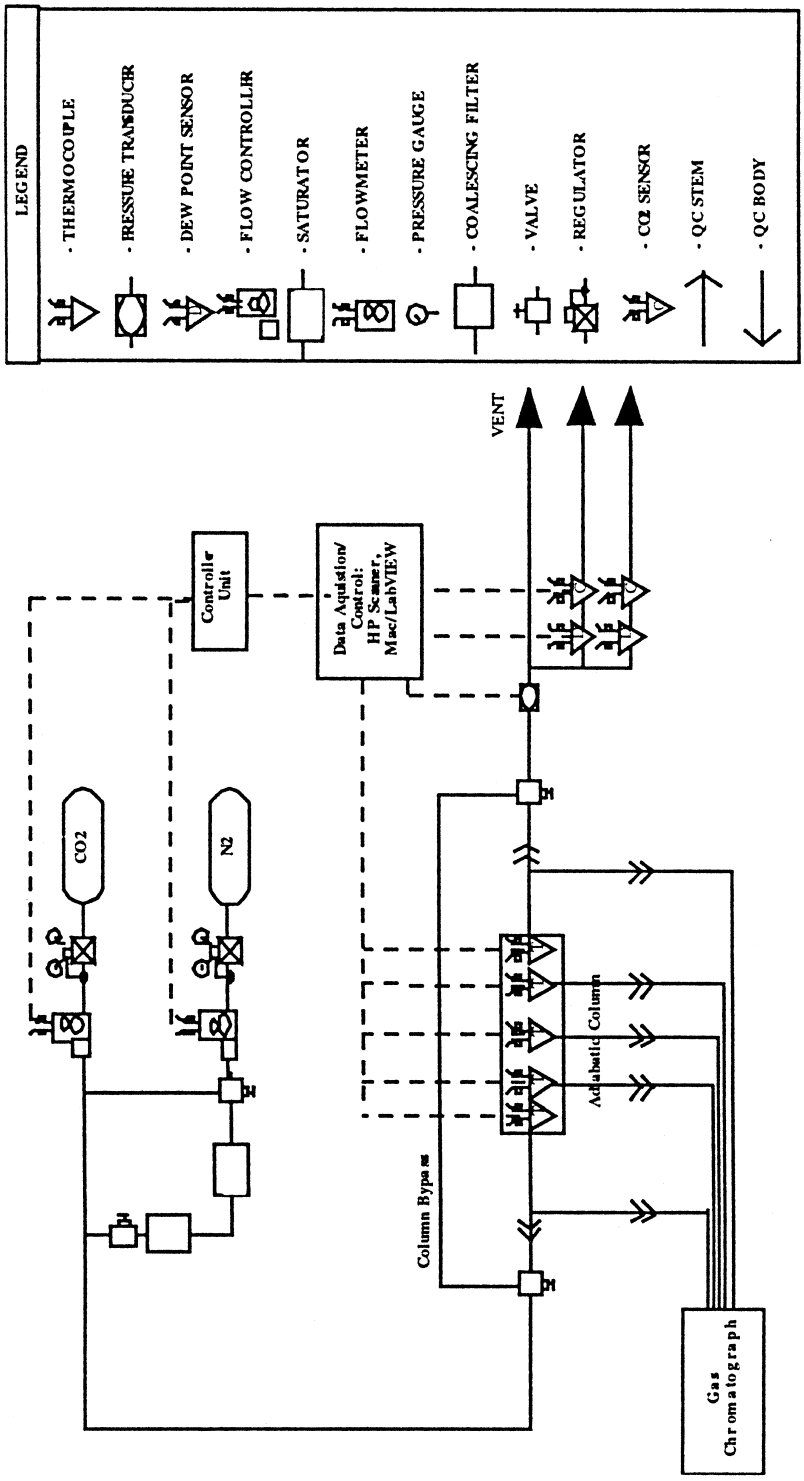

FIG. 1 Adsorption test system.

MARCEL DEKKER, INC.
270 Madison Avenue, New York, New York 10016

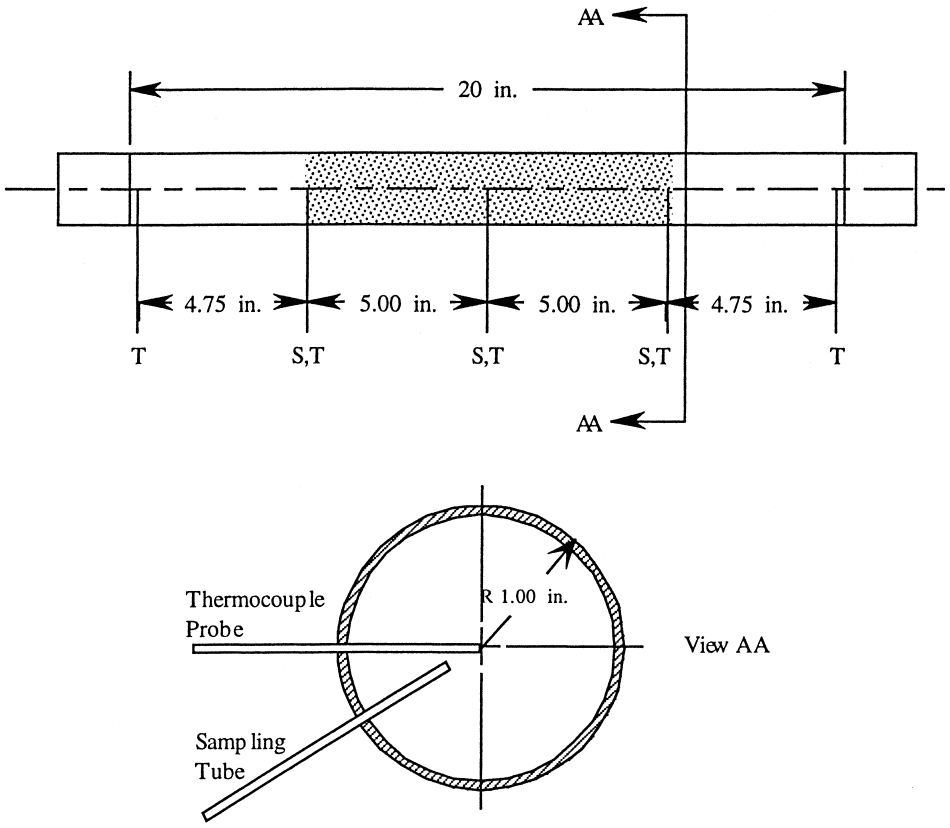

FIG. 2 Column sensor and sampling tube location.

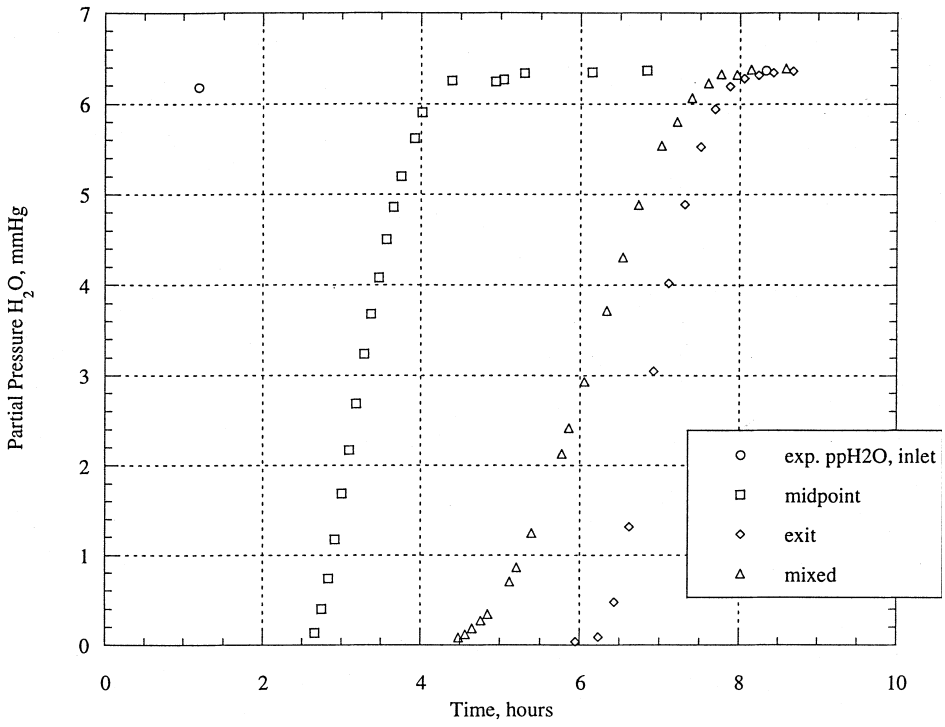

FIG. 3 H_2O breakthrough for $CO_2/H_2O/N_2$ coadsorption.

MARCEL DEKKER, INC.
270 Madison Avenue, New York, New York 10016

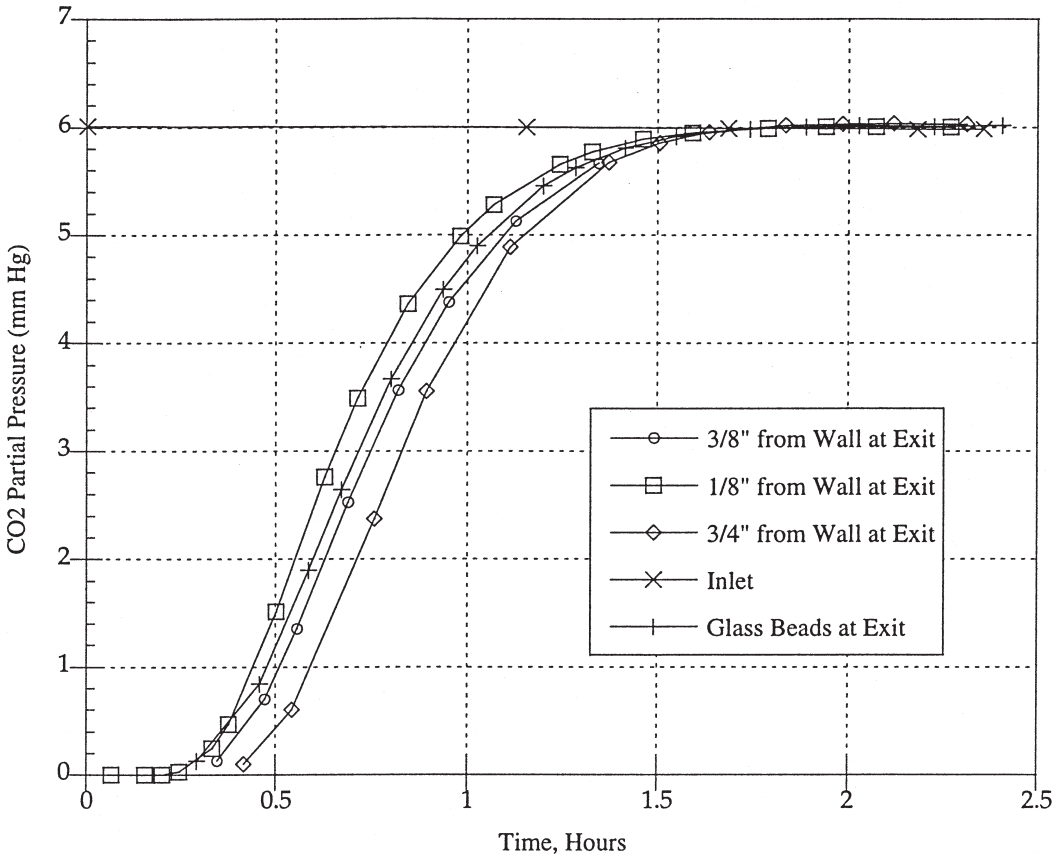

FIG. 4 CO_2 breakthrough for various radial positions.

ferent radial positions. The test results, shown in Fig. 4 show a clear relationship between concentration and radial position. As observed for H_2O breakthrough results, these results indicate greater permeability near the column wall. Since the heater core of the 4BMS (Four Bed Molecular Sieves) sorbent bed consists of channels roughly 0.5 inch in diameter, the channeling effect on CO_2 removal will likely be significant. The results of the two-dimensional model presented in a later paper (7) also confirm that channeling has a significant effect on this adsorption process.

MATHEMATICAL MODEL

Gas/Solid Equilibrium

The model discussed here was developed using equilibrium data provided by W. R. Grace & Co. (8). Nitrogen adsorption was represented with the Langmuir expression:

$$q_i^* = \frac{q_{mi} B_i P_i}{1 + B_i P_i} \quad (1)$$

Carbon dioxide and water adsorptions were correlated by the Langmuir–Freundlich equation (9):

$$q_i^* = \frac{q_{mi} B_i P_i^{n_i}}{1 + B_i P_i^{n_i}} \tag{2}$$

Two approaches were used to solve for the amounts of gases adsorbed in the solid phase in equilibrium with the gas-phase concentrations for multiple components. For simulations with N_2 and CO_2, the solution was obtained by an iterative procedure with the ideal adsorption solution theory (IAST) of Myers and Prasusnitz (10). For the case of the Langmuir–Freundlich single component isotherm, one gets

$$\sum_{i=1}^{i=n} \frac{Py_i}{\left(\dfrac{\exp\left(\dfrac{\pi A n_i}{RT q_{mi}} \right) - 1}{B_i} \right)^{1/n_i}} - 1 = 0 \tag{3}$$

Knowing the total pressure and the solid temperature, a value for the spreading pressure p is estimated, and solution will be obtained by iteration until Eq. (3) is satisfied. For the simulations with N_2, H_2O, and CO_2, the approach based on the Langmuir–Freundlich equation for multicomponent systems was found to give a more accurate results than the IAST model based on the nonideality of CO_2/H_2O. A paper is in the process for submission to discuss in details the use of IAST and Langmuir–Freundlich on the adsorption of CO_2/N_2 and $H_2O/CO_2/N_2$ on molecular sieve 5A:

$$q_i^* = \frac{q_{mi} B_i P_i^{n_i}}{1 + \sum_j B_j P_j^{n_j}} \tag{4}$$

The favorable agreement of simulation and test results using these correlations indicates low sensitivity to limitations of these correlations for components with differing adsorptivities. However, work continues toward a comprehensive gas/solid equilibrium model. For example, at low humidity levels, IAST accurately predicts multicomponent adsorption equilibria for CO_2 and H_2O. At higher humidity levels, CO_2 adsorption is underpredicted, as discussed by Finn (11).

Mass Balance Equation

In the bulk stream of the gas within the bed, the material balance for the adsorbate concentration is

$$\frac{\partial C_i}{\partial t} = D_l \frac{\partial^2 C_i}{\partial x^2} - \frac{\partial u C_i}{\partial x} - \frac{1 - \varepsilon}{\varepsilon} \frac{\partial \overline{q}_i}{\partial t} \tag{5}$$

Boundary and initial conditions:

$$\begin{aligned} &\text{at } t < 0,\ C_i = C_{i,0} \text{ for } 0 \le x \le L \\ &\text{at } t < 0,\ \bar{q}_i = \bar{q}_{i,0} \text{ for } 0 \le x \le L \\ &\text{at } t \ge 0,\ C_i = C_{i,0} \text{ for } x = 0 \\ &\text{at } t \ge 0,\ \partial C_i/\partial x = 0 \text{ for } x = L \end{aligned} \tag{6}$$

The axial diffusion, D_l, was calculated using an equation from Edward and Richardson's equation (12).

Assuming the ideal gas law $C_i = P/RT$ and knowing $\sum y_l = 1$, the above equation can be recast into an overall mass balance equation:

$$\begin{aligned} \frac{\partial P}{\partial t} = D_l \frac{\partial^2 P}{\partial x^2} - u\frac{\partial P}{\partial x} - P\frac{\partial u}{\partial x} \\ + \frac{P}{T_g}\left(\frac{\partial T}{\partial t} - D_l \frac{\partial^2 T}{\partial x^2} + u\frac{\partial T}{\partial x}\right) - RT\frac{1-\varepsilon}{\varepsilon}\sum_{i=1}^{n}\frac{\partial \bar{q}_i}{\partial t} \end{aligned} \tag{7}$$

This equation was used to compute axial velocity in the bed.

Gas-Phase Energy Equation

The change of gas temperature with respect to time is due to heat flux from the solid to the gas plus convection of heat due to the fluid flow, as shown by

$$\begin{aligned} \rho_g c_{pg}\frac{\partial T_g}{\partial t} = k_f \frac{\partial^2 T_g}{\partial x^2} - u\rho_g c_{pg}\frac{\partial T_g}{\partial x} \\ + \frac{1-\varepsilon}{\varepsilon} h_s a_s (T_s - T_g) - \frac{4h_w}{\varepsilon d}(T_g - T_w) \end{aligned} \tag{8}$$

Boundary and initial conditions:

$$\begin{aligned} &\text{at } t < 0,\ T_g = T_{g,0} \text{ for } 0 \le x \le L \\ &\text{at } t \ge 0,\ T_g = T_i \text{ for } x = 0 \\ &\text{at } t \ge 0,\ \partial T_g/\partial x = 0 \text{ for } x = L \end{aligned} \tag{9}$$

Note that T_w is calculated in Eq. (12).

Solid-Phase Energy Equation

The energy equation for the solid phase includes the term for heat flux from the solid phase to the gas phase plus heat generation due to adsorption:

$$\rho_s c_{ps}\frac{\partial T_s}{\partial t} = k_s \frac{\partial^2 T_s}{\partial x^2} + h_s a_s (T_g - T_s) - \sum_{i=1}^{n}\Delta H_i \frac{\partial \bar{q}_i}{\partial t} \tag{10}$$

Boundary and initial conditions:

$$\begin{aligned} &\text{at } t < 0,\ T_s = T_{s,0} \text{ for } 0 \le x \le L \\ &\text{at } t \ge 0,\ T_s = T_i \text{ for } x = 0 \\ &\text{at } t \ge 0,\ \partial T_s/\partial x = 0 \text{ for } x = L \end{aligned} \tag{11}$$

Column Wall Energy Equation

The wall temperature T_w is given by

$$\rho_w C_{pw} \frac{\partial T_w}{\partial t} = 2\pi R_i h_w (T_g - T_w) - 2\pi R_0 h_0 (T_w - T_0) \tag{12}$$

Initial condition:

$$\text{at } t < 0,\ T_w = T_{w,0} \tag{13}$$

Axial conduction is neglected since the area of heat transfer from the fluid to the wall is an order of magnitude larger than the area in the axial direction. This is analogous to heat conduction in a slab.

Momentum Equation

The Ergun equation (13, 14) is used to estimate the pressure drop:

$$\frac{dP}{dx} = -\frac{\mu}{K} u - \rho C u^2 \tag{14}$$

where C is the inertial coefficient. The empirical coefficients K and C are given by relations developed by Ergun for flow in a packed bed of spherical particle:

$$K = \frac{d^2 \varepsilon^3}{150(1-\varepsilon)^2} \tag{15}$$

$$C = \frac{1.75(1-\varepsilon)}{d\varepsilon^3} \tag{16}$$

Using gas velocity as calculated in Eq. (7) the total pressure was found with Eq. (14).

Solid-Phase Transport Equation

Mass transfer of solute from the bulk gas to sorbed state is driven by the difference in the actual adsorbed quantity versus the quantity that would be adsorbed at equilibrium conditions. In general, the mass transfer mechanism of an adsorption process includes four steps: fluid-film diffusion, pore diffusion,

adsorption rate, and surface diffusion. Adsorption rate can be neglected since it is much greater than the diffusion rates as discussed by Yang (15).

Zeolite sorbents consist of crystals, in the 1–9 μm size range, which are pelletized with a small amount of binder. Macropore (spaces between the crystals) and micropore (intracrystalline) diffusion must in general be considered. However, for molecules in the size range of CO_2 adsorbing onto 5A zeolite, the diffusion rate inside the pellet has been shown to be controlled by intracrystalline diffusion (16).

Assuming the intracrystalline diffusion governs the overall mass transfer, the linear driving force (LDF) model based on Glueckauf, (17) may be used:

$$\partial \bar{q}_i/\partial t = k_{\text{ef}} a_s (q_i^* - \bar{q}_i) \tag{17}$$

where k_{ef} is obtained by experimental procedure and a_s is the interfacial surface area. The justification of assuming a linear diving force to model the adsorbed concentration in the solid phase has been well established by other researchers; for example, the authors of References 16, 21, 22, and 23, to name a few.

Gas to pellet heat transfer coefficients obtained from Petrovic and Thodos (18), for CO_2, H_2O, and N_2 were .0875, .1002, and .0844 cm/s, respectively. The empirically obtained mass transfer coefficients using the LDF model for CO_2, H_2O, and N_2 were 1.27×10^{-4}, 2.625×10^{-5}, and 3.75×10^{-4} cm/s, respectively. Since the overall mass transfer rate is three orders of magnitudes smaller than the calculated mass transfer rate from the gas phase to the pellet surface, the latter was neglected.

Numerical Solution

The solution of this system must be obtained numerically. For an n component mixture, the numerical model will require the solution of several coupled differential equations: $n - 1$ mass balance equations, n rate equations and equilibrium isotherms, the overall mass balance equation, the momentum equation, and the heat balance equation each for the fluid phase, gas phase, and column wall.

In this work the PDEs were discretized using the finite difference method. The first-order approximation was used for the time dimension. First-order boundary nodes and second-order internal nodes were used for spacial coordinates. The set of discretized finite difference equations was solved simultaneously by an implicit method. The method of Newman (19, 20) was found to be effective for the steep gradient of mass concentration along the bed length.

Fifty nodes represented the column length. The time step was increased from 3.6 to 60 seconds as the solution progressed. Convergence was assumed when $(C^{n+1} + C^n)/C^{n+1}$ was less than 1.0×10^{-4} for each grid point. Here C is the gas phase concentration, n indicates the previous time step, and $n + 1$ the current time step.

RESULTS

In this section we present modeling results which illustrate the importance of accurately simulating critical adsorption processes, and comparisons of model results with test data. Simulations were performed on an ALPHA VAX computer. Experiments were performed on the insulated fixed-bed rig at MSFC. The sorbent was a 5A zeolite. Nitrogen was the carrier gas. Experiments begin with the column at ambient room temperature.

Thermal Effects Modeling

Heat transfer coefficients are found by comparison of the thermal model with heating of the subscale column with an inert gas, shown in Fig. 5.

Nitrogen was heated to a temperature of 350°F and passed through an initially cold column. The markers are the measured temperatures at the inlet, midpoint, and exit of the column. The lines are the results from simulation.

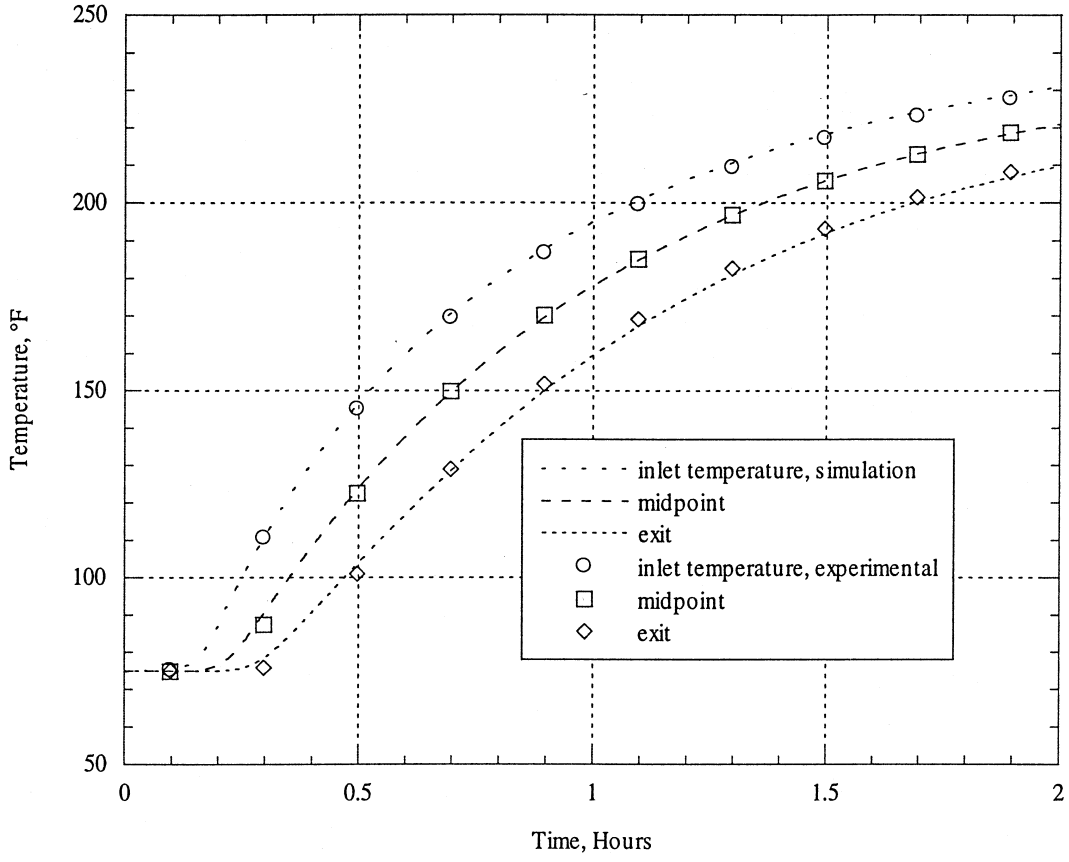

FIG. 5 Thermal model validation.

MARCEL DEKKER, INC.
270 Madison Avenue, New York, New York 10016

Resultant heat transfer coefficients are 2.5 Btu/h·ft^2 from the fluid stream to the canister wall, and 0.25 Btu/h·ft^2 from the canister wall to the atmosphere. These values are used in the simulations described below.

Nitrogen Coadsorption Effects Modeling

The importance of not neglecting the nitrogen coadsorption with CO_2 is shown in Fig. 6. CO_2 in nitrogen at 6.2 mmHg was passed through an initially clean zeolite column. The gas at the column centerline was analyzed periodically at the column inlet, midpoint, and outlet. These results are compared with simulations that either included (solid lines) or neglected (dashed lines) the effect of nitrogen. Nitrogen clearly has a noticeable effect; however the simulations that included N_2 adsorption overpredicted the effect slightly.

The thermal sensitivity to N_2 coadsorption is shown in Fig. 7. The agreement is much better when the heat of adsorption of nitrogen is included. A decrease in temperature occurs at 0.15 hours in both the test data and the simulation, due to N_2 displacement by CO_2, and N_2 reduces the bed capacity and lowers the overall bed temperatures through desorption.

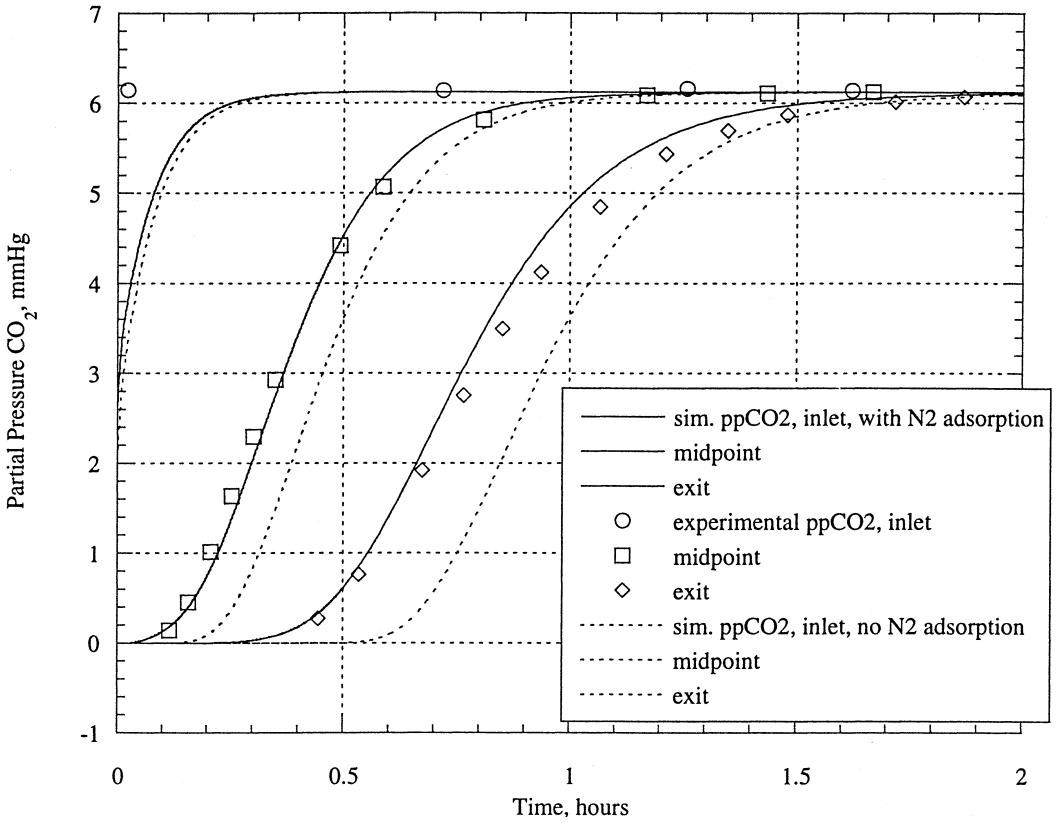

FIG. 6 Effect of nitrogen coadsorption on CO_2 breakthrough.

MARCEL DEKKER, INC.
270 Madison Avenue, New York, New York 10016

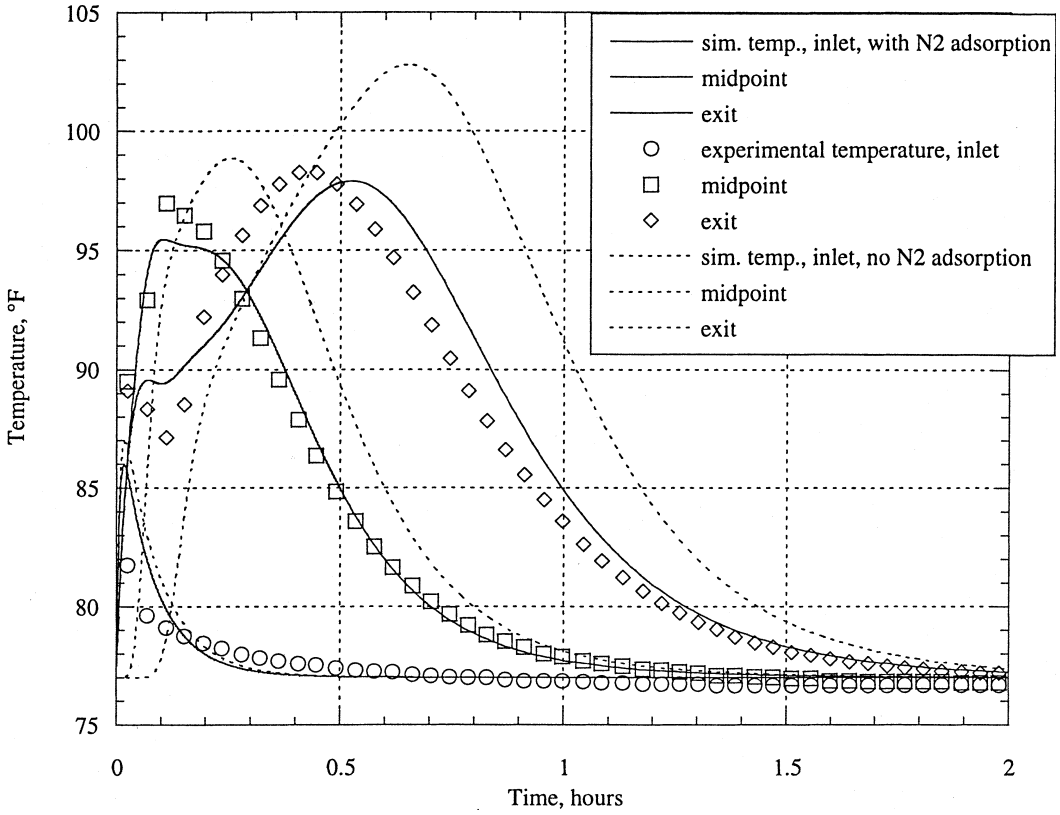

FIG. 7 Heat transfer effect of nitrogen coadsorption.

Water Coadsorption Effects Modeling

Verification of the model for $CO_2/H_2O/N_2$ coadsorption is shown in Figs. 8 to 10. These three figures illustrate testing and simulation runs for adsorption of water at 6.3 mmHg and CO_2 at 2.89 mmHg in a carrier gas of nitrogen. All figures show test data as markers and simulation data as lines.

Figure 8 illustrates the roll-up phenomenon as adsorbed CO_2 is driven off by water and the CO_2 partial pressure rises above the inlet level temporarily. The effect should be larger at the column outlet than midpoint as shown by test data.

Figure 9 shows the water breakthrough at the column midpoint and outlet. Also shown is the H_2O partial pressure of gas mixed by passing through glass beads downstream of the sorbent material. Note the mixed gas breaks through before the gas at the centerline, indicating that channeling is significant along the walls of the 2-inch diameter column. Since the heater core of the 4BMS sorbent bed consists of channels roughly 0.5 inch in diameter, the channeling effect on CO_2 removal will be significant. The results of the two-dimensional model (not shown here) confirm that channeling has a significant effect on this

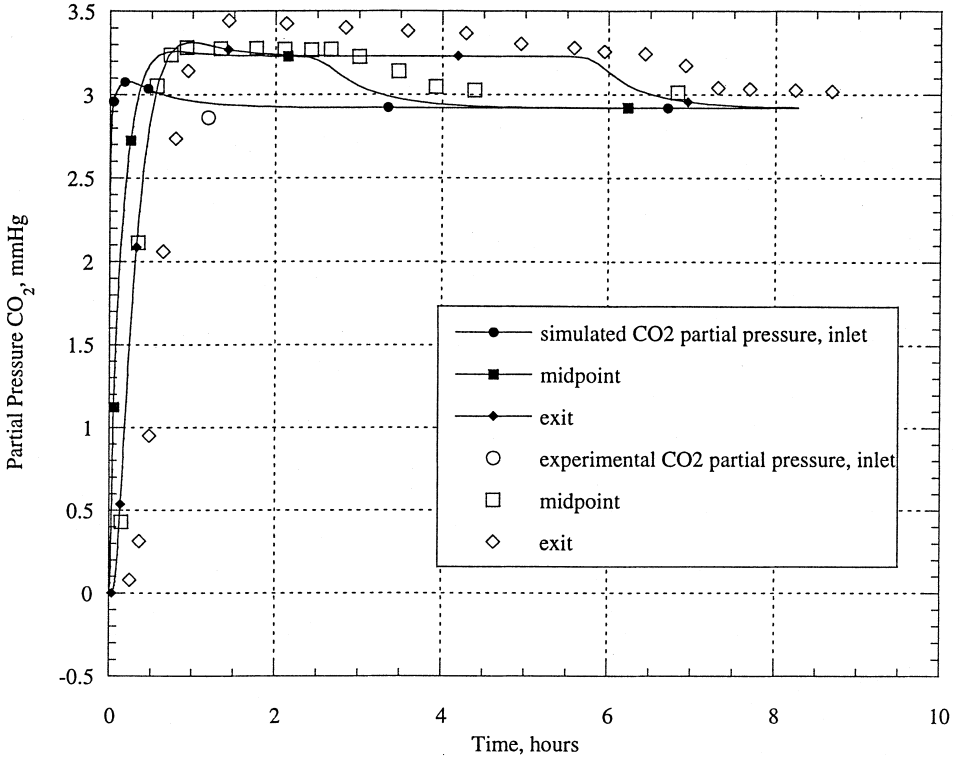

FIG. 8 CO_2 breakthrough for $CO_2/H_2O/N_2$ coadsorption.

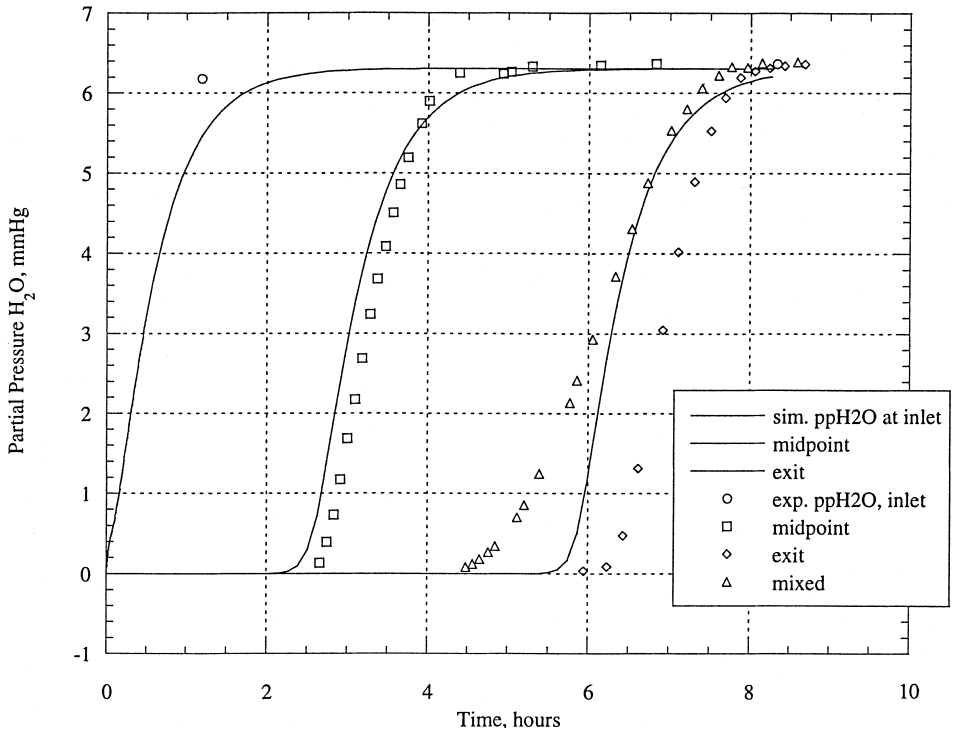

FIG. 9 H_2O breakthrough for $CO_2/H_2O/N_2$ coadsorption.

MARCEL DEKKER, INC.
270 Madison Avenue, New York, New York 10016

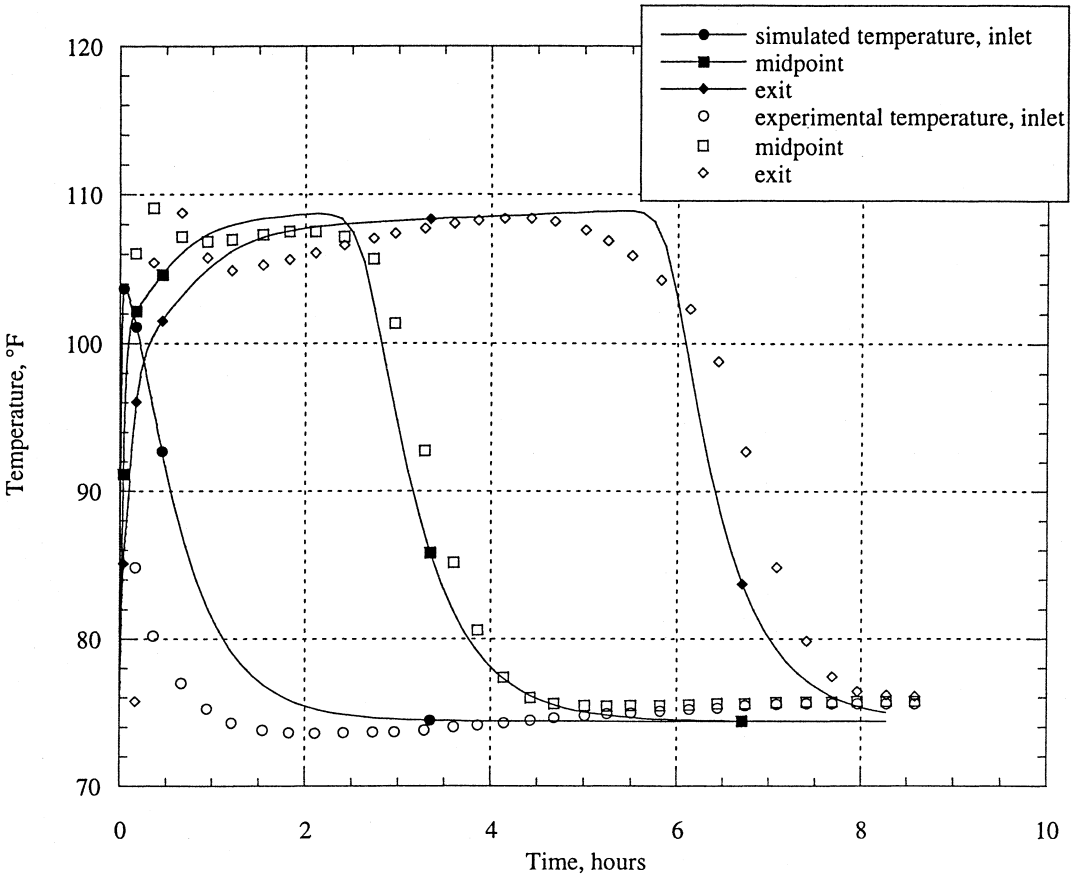

FIG. 10 Heat transfer for $CO_2/H_2O/N_2$ coadsorption.

adsorption process. Finally, Fig. 10 shows the temperatures of the bed at midpoint and outlet.

Bed Regeneration

Desorption of CO_2 test results in comparison with the model are shown by the solid lines in Figs. 11 and 12. After the bed was saturated with CO_2, the regeneration process was started by using N_2 as the purge gas. As it shown, the effluent concentration of CO_2 has a sharp drop in the first few minutes and the slope of the breakthrough flattens out as time goes by. The initial drop in temperature is due to heat of desorption and finally reaches the inlet condition when there is no depletion of CO_2 from the bed. The same mass transfer coefficient of 0.017 was used. The model predicts both temperature and breakthrough fairly well. The LAST was used to predict the mixture isotherm of CO_2/N_2

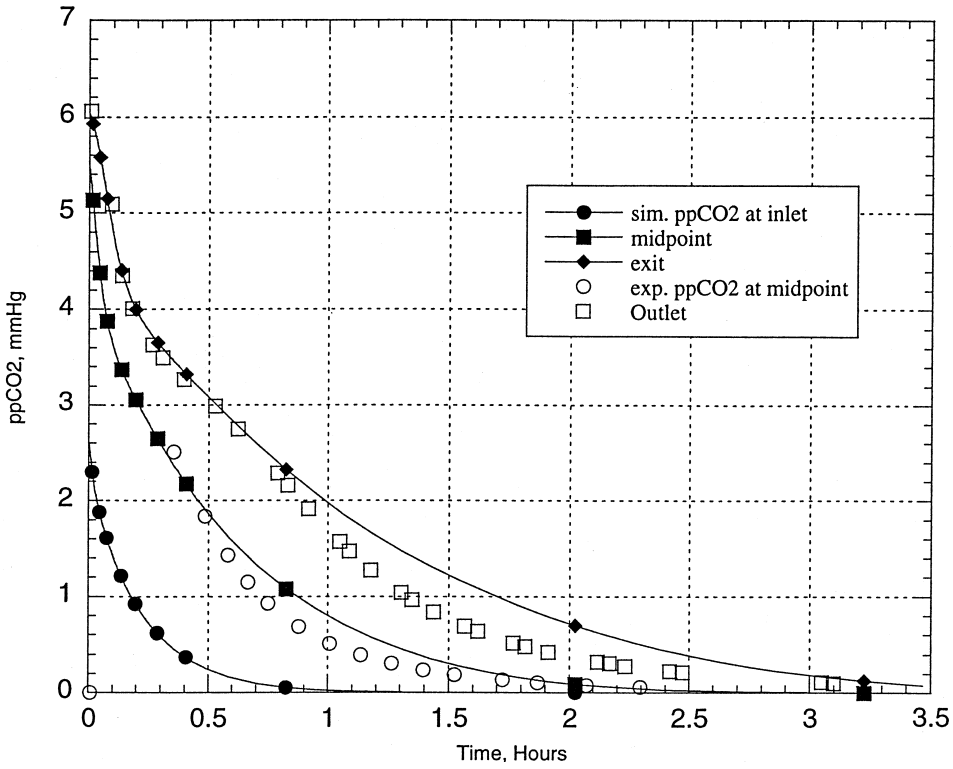

FIG. 11 CO_2 depletion for CO_2/N_2 desorption.

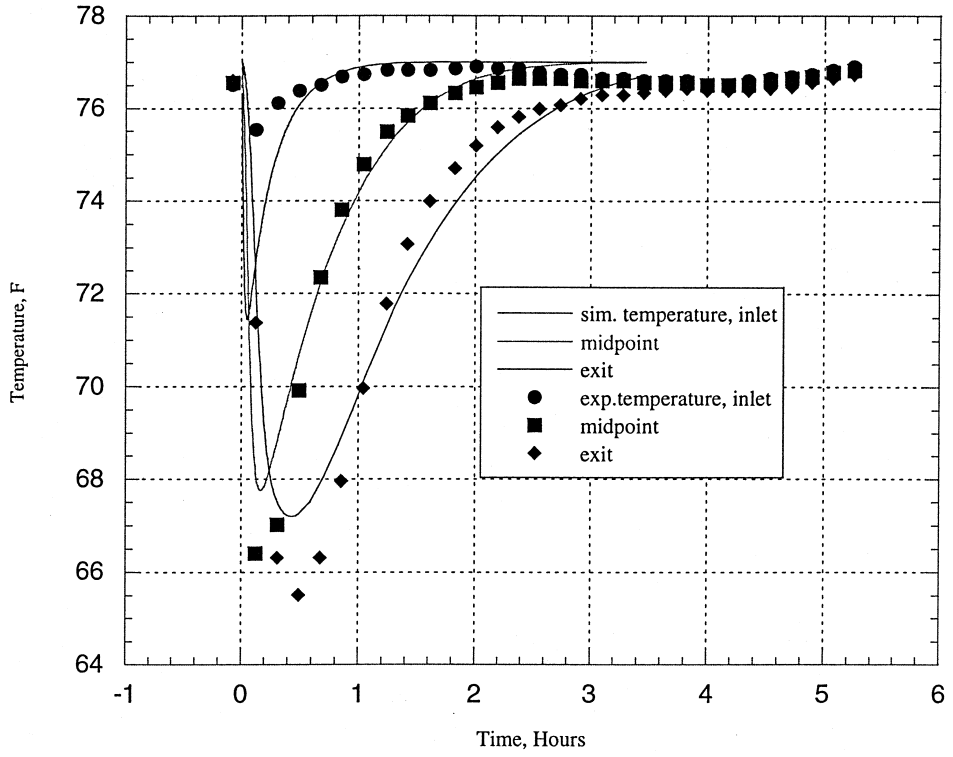

FIG. 12 Heat transfer effects of CO_2 depletion for CO_2/N_2 desorption.

MARCEL DEKKER, INC.
270 Madison Avenue, New York, New York 10016

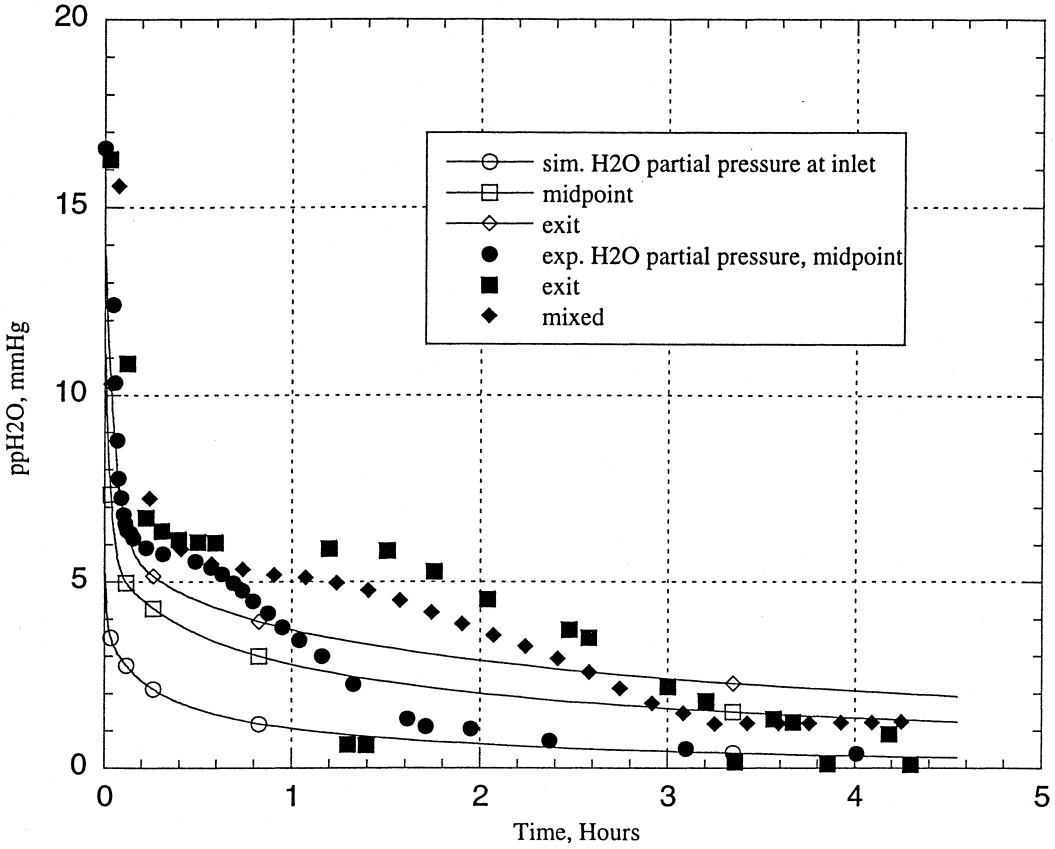

FIG. 13 H_2O depletion for H_2O/N_2 desorption.

Desorption of H_2O test results in comparison with the model are shown by the solid lines in Figs. 13 and 14. The results of the partial pressure of H_2O and the temperature profile of this one-dimensional desorption model are not in good agreement with the test data. The model shows a fast reduction of H_2O partial pressure in the gas phase. A mass transfer coefficient as large as 0.04 ft/h, in contrast with 0.0035 ft/h in the case of H_2O adsorption, was used. Generally, there should not be such a large difference between the two coefficients. Even with this large mass transfer coefficient, the desorption of H_2O from the bed was insufficient to increase the H_2O partial pressure in the gas phase. In contrast with the adsorption process, any small discrepancy of H_2O partial pressure with test data will remain as a error throughout the completion of the test. In adsorption any small error at any point in the bed, if it is caused by the isotherm at some partial pressure of the feed, will be eliminated at a later time because of the correct isotherm value at a larger partial pressure of the feed. This can be seen from the early breakthrough observed by other researchers. The obvious reason is that the equilibrium isotherm at low partial

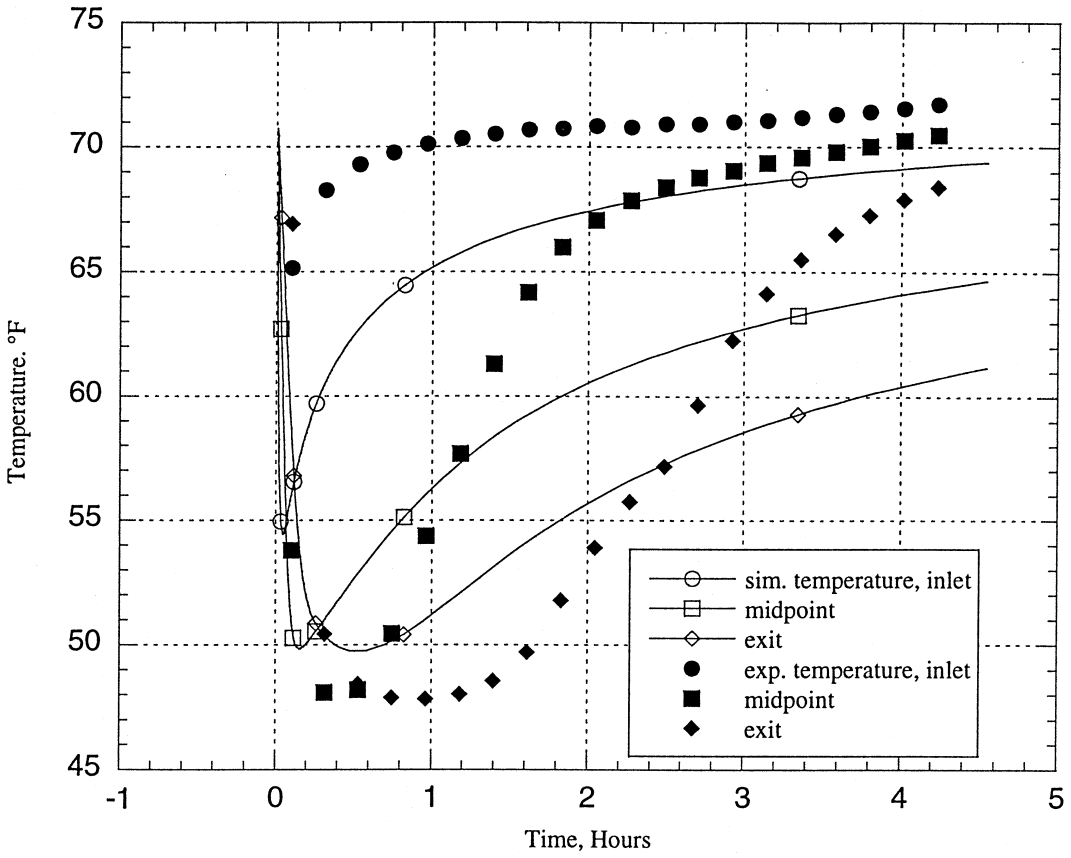

FIG. 14 Heat transfer effects of H_2O depletion for H_2O/N_2 desorption.

pressures are being underestimated. It is also possible that the equilibrium isotherm of H_2O on 5A material shows hysteresis so that the apparent equilibrium pressures observed in adsorption and desorption experiments are different. The concentration of a key component, CO_2, is affected by the presence of the nonkey component, N_2, in CO_2/N_2 adsorption. CO_2 effluent concentration overshoots its inlet concentration because of H_2O displacement (more easily adsorbed component). The height of this roll-up is increased with the inlet concentration of the H_2O component. The most significant contribution to the difference in model and experimental results of H_2O desorption depends on the fact that the duration of an H_2O adsorption run takes about 15 hours for completion of a test. Also, the desorption run duration takes 10 to 12 hours. During this long duration the temperature of the location where the test took place varied about 10 to 15°F during the night. This in turn affects the saturated air that was used to saturate the column. Therefore, it is accurate to conclude the amount of H_2O adsorbed on the bed is less than what is assumed in the model.

On the basis of the data presented here, and other comparisons between desorption test data and simulation results not yet published, this computer model meets its primary objective—achieving predictive capability. Enhancements to the model as discussed should increase its accuracy. Efforts are continuing to develop on the integrated 4BMS simulation, equilibrium isotherms, heat and mass transfer coefficients, and verification data.

CONCLUSIONS

Based on analytical and experimental investigation of convective flows in porous media, the following conclusions are drawn:

- The experimental results from the laboratory-scale, fixed-bed adsorber are quantitatively consistent with the one-dimensional model at the column center. The average concentration of a cross-sectional bed obtained by test results deviates from the column center concentration appreciably. This indicates the strong effects of porosity variation along the radial direction of the column bed on the temperature, concentration, and velocity field. Results from the model were encouraging and contributed to the decision to model the dynamic behavior of the column in two dimensions.
- A linear driving force mass transfer model provides a reasonable fit to experimental adsorption data.
- The concentration of a key component, CO_2, is affected by the presence of the nonkey component, N_2, in CO_2/N_2 adsorption. CO_2 effluent concentration overshoots its inlet concentration because of H_2O displacement (more easily adsorbed component). The height of this roll-up is increases with the inlet concentration of the H_2O component.

NOMENCLATURE

A	surface area of pellets per unit volume of pellet (ft^2/ft^3) surface area (ft^2)
B	Langmuir constant
C	constant in Darcy equation gas stream concentration ($lb \cdot mol/ft^3$)
c_{ip}	gas-phase concentration of ith component in the gas stream ($lb \cdot mol/ft^3$)
$C_{i,0}$	gas-phase concentration of ith component at boundary or initial ($lb \cdot mol/ft^3$)
C_{pg}	heat capacity of gas phase ($Btu/lb_m \cdot R$)

MARCEL DEKKER, INC.
270 Madison Avenue, New York, New York 10016

C_{ps} heat capacity of solid particle (Btu/lb_m·R)
C_{pw} heat capacity of column wall (Btu/lb_m·R)
D diffusivity (ft^2/h)
D_l axial diffusion (ft^2/h)
H_0 effective heat transfer coefficient for column insulation (Btu/ft^2·h)
H_w heat transfer coefficient between the gas stream and the column wall (Btu/ft^2·h)
H_s heat transfer coefficient between the gas stream and the sorbent (Btu/ft^2·h)
ΔH heat of adsorption (Btu/lb·mol)
K constant in Darcy equation
k_e mass transfer coefficient (ft/h)
K_f axial conductivity of fluid flow (Btu/ft·h·R)
K_s solid thermal conductivity (Btu/ft·h·R)
M_i molecular weight of adsorbate i (lb/lb·mol)
N number of components
P total pressure (mmHg or lb_f/ft^2)
P_i partial pressure of component i (mmHg or lb_f/ft^2)
q_i^* solid-phase concentration of ith component in equilibrium with gas phase (lb·mol/ft^3 of solid)
q_{mi} Langmuir constant
R ideal gas constant (555 mmHg·ft^3/lb·mol·R)
R_i inside wall diameter of column (ft)
R_0 outside wall diameter of column (ft)
R_p particle radius (ft)
t time (h)
T temperature (R)
T_0 ambient temperature (R)
T_g gas temperature (R)
T_w wall temperature, R
T_s Solid temperature (R)
U interstitial velocity (ft/h)

Greek Letters

ε external bed void volume
ρ_{pg} density of gas phase (lb·mol/ft^3)
ρ_s density of solid phase (lb/ft^3)
ρ_w density of column wall (lb·mol/ft^3)
π constant or spreading pressure
ΔH heat of adsorption (Btu/lb of solid)

MARCEL DEKKER, INC.
270 Madison Avenue, New York, New York 10016

Subscripts

i	*i*th component
e	effective
0	outside, initial
pg	gas phase
ps	solid phase
s	surface
t	total
w	wall

Superscripts

−	average value
*	equilibrium value

REFERENCES

1. D. A. Nield, "Alternative Model for Wall Effect in Laminar Flow of Fluid through a Packed Column," *AIChE J*., *29*, 688 (1983).
2. Y. Cohen and A. B. Metzner, "Wall Effect in Laminar Flow of Fluids through Packed Beds," *Ibid*., *27*, 705 (1981).
3. C. F. Chu and K. M. Ng, "Flow in Packed Tubes with a Small Tube to Particle Diameter Ratio," *Ibid*., *35*, 148–158 (1989).
4. J. Tobis and D. Vortmeyer, "Near Wall Channeling Effect on Isothermal Constant-Pattern Adsorption," *Chem*. *Eng*. *Sci*., pp. 1363–1369 (1988).
5. P. Cheng and H. Zhu, "Effects of Radial Thermal Dispersion on Fully-Developed Forced Convection in Cylindrical Packed Tubes," *J*. *Heat Mass Transfer*, *30*, 2373–2383 (1987).
6. D. E. Beasley and J. A. Clark, "Transient Response of a Packed Bed for Thermal Energy Storage," *Ibid*., *27*, 1659–1669 (1984).
7. H. Mohamadinejad and J. C. Knox, Submitted to *Separation Science and Technology*.
8. *Davison Molecular Sieves Adsorption Equilibria*, Davison Chemical Division, W. R. Grace & Co., Baltimore, Maryland.
9. I. Langmuir, "The Adsorption of Gases on Plane Surface of Glass, Mica, Platinum," *J*. *Am*. *Chem*. *Soc*., *40*, 1361 (1918).
10. A. L. Myers and J. M. Prausnitz, "Thermodynamics of Mixed-Gas Adsorption," *AIChE J*., *11*, 121 (1965).
11. J. E. Finn, *4BMS Adsorption Characterization Project Status Report*, Ames Research Center, Moffet Field, California, 1996.
12. M. F. Edwards and J. F. Richardson, "Gas Dispersion in Packed Beds," *Chem*. *Eng*. *Sci*., *23*, 109 (1968).
13. S. Ergun, "Fluid Flow through Packed Column," *Chem*. *Eng*. *Prog*., *48*, 89–94 (1952).
14. G. S. Beavers and E. M. Sparrow, "Non-Darcy Flow through Fibrous Porous Media," *J*. *Appl*. *Mech*., *36*, 711–714 (1969).
15. R. T. Yang, *Gas Separation by Adsorption Process*, Butterworths, Boston, MA, 1987.
16. D. M. Ruthven, *Principle of Adsorption and Adsorption Processes*, Wiley, New York, NY, 1984.

17. E. Glueckauf, "Theory of Chromatography—Part 10," *Trans. Faraday. Soc., 51,* 1540 (1955).
18. L. J. Petrovic and G. Thodos, "Mass Transfer in the Flow of Gases through Packed Bed," *Ind. Eng. Chem. Fundam., 7*(2), 274 (1968).
19. J. Newman, *Numerical Solution of Coupled, Ordinary Differential Equations* (UCRL-17739), Lawrence Radiation Laboratory, University of California, Berkeley, August 1967.
20. J. Newman, "Numerical Solution of Coupled, Ordinary Differential Equations," *Ind. Eng. Chem. Fundam., 7*, 514–517 (1968).
21. D. D. Do, "Sorption of Bimodal Microporous Solids with an Irreversible Isotherm," *Chem. Eng. Sci., 44*(8), 1707–1713 (1989).
22. D. R. Grag and D. M. Ruthven, "The Effect of Concentration Dependence of Diffusivity on Zeolitic Sorption Curves," *Ibid., 27*, 417–423 (1972).
23. R. W. H. Sargent and C. J. Whitford, "Diffusion of Carbon Dioxide in Type 5A Molecular Sieve," in *Molecular Sieve II* (Advances in Chemistry Series 102), American Chemistry Society, Washington, DC, 1971.

Received by editor November 17, 1998
Revision received May 1999

Request Permission or Order Reprints Instantly!